




Shedding light on *Paraconiothyrium brasiliense*: Secondary metabolites, biological activities, and computational studies

Sabrin R. M. Ibrahim^{1*}, Abdulrahim A. Alzain², Fatima A. Elbadwi², Abdulrahman E. Koshak³, Aram Hamad AlSaedi⁴, Ahmed Ashour⁵, Wadah Osman⁵, Ikhlas A. Sindi⁶, Selwan M. El-Sayed⁷, Abdelbasset A. Farahat⁸, Ahmed H.E. Hassan⁷, Gamal A. Mohamed³

¹Preparatory Year Program, Department of Chemistry, Batterjee Medical College, Jeddah, Saudi Arabia.

²Department of Pharmaceutical Chemistry, Faculty of Pharmacy, University of Gezira, Wad Madani, Sudan.

³Department of Natural Products and Alternative Medicine, Faculty of Pharmacy, King Abdulaziz University, Jeddah, Saudi Arabia.

⁴College of Medicine, Taibah University, Medina, Saudi Arabia.

⁵Department of Pharmacognosy, Faculty of Pharmacy, Prince Sattam Bin Abdulaziz University, Al Kharj, Saudi Arabia.

⁶Department of Biology, Faculty of Science, King Abdulaziz University, Jeddah, Saudi Arabia.

⁷Department of Medicinal Chemistry, Faculty of Pharmacy, Mansoura University, Mansoura, Egypt.

⁸Master of Pharmaceutical Sciences Program, California Northstate University, Elk Grove, CA.

ARTICLE HISTORY

Received on: 09/05/2024

Accepted on: 03/08/2024

Available Online: 05/10/2024

Key words:

Paraconiothyrium brasiliense, secondary metabolites, bioactivities, sustainable development goals, life on land, molecular docking, ADMET prediction.

ABSTRACT

Fungi are renowned as a prolific source for the biosynthesis of therapeutically valuable metabolites. *Paraconiothyrium* genus (Leptosphaeriaceae) demonstrates remarkable potential for the biosynthesis of a wide array of metabolites, including macrolides, terpenoids, polyketides, phenolics, and furanones, which exhibit diverse bioactivities. The present review focused on the reported metabolites derived from *Paraconiothyrium brasiliense*, including their chemical structures and bioactive properties. Furthermore, it delves into the elucidation of the biosynthetic pathways for these metabolites. This review encompasses the description of over 92 compounds reported in the literature from 2010 to October 2023. In addition, *in silico* studies may explain the potential mechanisms underlying the neuroprotective properties of certain furanone derivatives against central nervous system disorders. Among the tested compounds against KEAP1 through Keap1/Nrf2 pathway-mediated neuroprotection, paraconifuranone I (**48**), paraconifuranone J (**50**), and paraconifuranone L (**51**) displayed docking scores ranging from −6.158 to −6.612 kcal/mol, similar to the exciting reference compound which achieved the highest docking score of −6.633 kcal/mol. Moreover, new potential activities of some compounds as inhibitors against the LasR target of *Pseudomonas aeruginosa* were elucidated using molecular docking and absorption, distribution, metabolism, excretion, and toxicity prediction. Specifically, 1-(1',2'-dideoxy- α -D-nucleopyranosyl)- β -carboline (**73**) had the highest docking score at −11.327 kcal/mol, followed by 1-acetyl- β -carboline (**75**) at −10.055 kcal/mol, in comparison to reference compound (docking score −10.023 kcal/mol). In addition, ten other compounds displayed competitive docking scores ranging from −9.813 to −9.312 kcal/mol. This suggested the potential of *P. brasiliense* as a promising lead for antibacterial and neuroprotective agents.

INTRODUCTION

Exploiting microorganisms, particularly fungi, has the promise to assist humanity in achieving the sustainable

development goals of the UN, assist in feeding the growing global population, and enhance the bio-economies of less developed countries [1]. Fungi are indispensable and essential constituents of the ecosystem [2]. They have irreplaceable contributions to the ecosystem such as nutrient cycling and decomposition of organic matter, as well as lessening the effects of climate change [3,4]. They are considered key players in the degradation of organic wastes because of their secreting enzymes' capability [5–7]. They have

*Corresponding Author

Sabrin R. M. Ibrahim, Preparatory Year Program, Department of Chemistry, Batterjee Medical College, Jeddah, Saudi Arabia.

E-mail: sabrin.ibrahim@bmc.edu.sa

been investigated for their capacity to produce bioplastics, biofuels, detergents, biosurfactants, and other bio-based materials that can contribute to a more sustainable and lower carbon economy and reduce greenhouse gas emissions [8–10]. In addition, fungi are a wealthy pool of structural unique metabolites with diverse bioactivities such as cytonic acids A and B (human cytomegalovirus protease inhibitors), hinnuliquinone (human immunodeficiency virus (HIV-1) protease inhibitor), paclitaxel (antineoplastic agent), isopestacin and pestacin (antioxidants), and lariatins A and B (anti-HIV) [11–14]. In addition, they represent a biosynthetic factory for discovering or synthesis of novel, high-value metabolites of notable potential in treating various disorders such as antifungals (e.g., echinocandins, caspofungin, anidulafungin, and micafungin), antibiotics (e.g., cephalosporin C, fusidic acid, and retapamulin), immunosuppressants (e.g., mycophenolic acid and mizoribine), and anti-hypercholesterolemic (e.g., mevastatin and lovastatin) [15]. Currently, some fungal metabolites are in clinical trials for chronic illnesses such as drug-resistant depression and cancer [15].

Paraconiothyrium genus (family: Sphaeropsidaceae; order Sphaeropsidales; class Coelomycetes) was discovered by Verkley *et al.* in 2004 [16–18], which belongs to Ascomycota with common species such as *Paraconiothyrium brasiliense*, *P. estuarinum*, *P. fungicola*, *P. variabile*, *P. hawaiiense*, and *P. cyclothyrioides* [19]. Species of the genus *Paraconiothyrium* are widely found as opportunistic human pathogens, endophytes, phytopathogens, saprophytism in soil and estuaries, and mycoparasitism, as well as in association with the insects' digestive tract [19–21]. This genus includes 27 species that have the capacity to produce diverse classes of metabolites, such as macrolides, diterpenoids, sesquiterpenoids, isoprenoids, polyketides, phenolics, and furanones, some of them demonstrated diverse bio-activities, including anti-HIV, cytotoxicity, and anti-fungal [16,20]. In 2021, a review by Wang *et al.* discussed the species, bioactivities, and secondary metabolites of *Paraconiothyrium* genus [22]. One of the most studied species of this genus is *P. brasiliense* Verkley which was described in Brazil from *Coffea arabica* fruits, from *Acer truncatum* in China, *Magnolia* sp. in Italy; *Prunus salicina* and *P. persica* in South Africa; *Vitis vinifera* in Spain; *Sarcococca saligna* in Pakistan [2,17,18,23]. Recently, it was first reported as a human and plant pathogenic fungus that causes eyelid cellulitis and leaf spots of *Sarcococca saligna*, respectively [23,24]. On the other side, this fungus produced structurally diverse metabolites such as terpenoids, octahydronaphthalenes, furanones, anthraquinones, xanthenes, isocoumarins, and alkaloids with valuable biological activities. It is noteworthy that a comprehensive review with a special focus on *P. brasiliense* has not been retrieved. This work aims to shed light on *P. brasiliense* from a poorly described genus, including its metabolites, bioactivities, and potential applications. In addition, the reported biosynthetic pathways of its major metabolites were discussed. Furthermore, the exploration of the bioactive potential of *P. brasiliense* metabolites extends beyond their known properties. Our investigation delves into the *in-silico* studies, offering unique insights into the underlying mechanisms

that govern the neuroprotective attributes exhibited by some paraconifuranones, particularly against central nervous system (CNS) disorders. Furthermore, our research endeavors reveal novel uses of these compounds by uncovering their potential as antibacterial inhibitors, specifically targeting *Pseudomonas aeruginosa*. By delving into these unexplored areas of these dual bioactive roles, our study not only furthers our understanding of the pharmacological potential of *P. brasiliense*-derived metabolites but also highlights their promising prospects in the fields of neuroprotection and antimicrobial therapy.

METHODOLOGY

The data were gathered through a search on various databases and publishers: Google-Scholar, Web of Science, Pub-Med, Sci-Finder, Scopus, Wiley, American Chemical Society, and SpringerLink Publications using keywords *P. brasiliense* + compounds; *P. brasiliense* + sesquiterpenoids; *P. brasiliense* + biological activity; *P. Brasiliense* + enzymes; *P. Brasiliense* + NPs.

PARACONIOTHYRIUM BRASILIENSE METABOLITES

Paraconiothyrium brasiliense was rarely chemically explored. Sesquiterpenoids and furanones are the principal metabolites reported from this fungus (Table 1). These metabolites were reported from the strains isolated from endophytic, insect, and sea sediments (Fig. 1). These metabolites along with their bioactivities were discussed below.

Sesquiterpenoids

Bergamotane-sesquiterpenoids

Bergamotane-sesquiterpenoids are among the commonly reported sesquiterpenes from this fungus [13]. In 2010, Liu *et al.* isolated and purified new bergamotane-sesquiterpenes: brasilamides A–D (1–4) and the known pinthunamide (14) from the *Acer truncatum*-associated strain M3–3341 obtained from Dongling Mountain/Beijing/China that were characterized by nuclear magnetic resonance (NMR), circular dichroism (CD), and Xray analyses (Fig. 2) [25]. Compounds 1 and 2 feature unique skeletons, including 4-oxatricyclo[3.3.1.0^{2,7}]nonane skeleton, with a tetrahydro-2H-pyran or a tetrahydro-2H-pyrone moiety connected to the bicyclo[3.1.1]heptane ring at C-5 and C-2. Compounds 3 and 4 are related to 14, they possess an unrivaled 9-oxatricyclo[4.3.0.0^{4,7}]nonane moiety with tetrahydrofuran moiety linked to a bicycle[3.1.1]heptane moiety instead of a γ -lactone ring and different substituents attached to C-10 [25].

In a study by Guo *et al.*, brasilamides K–N (5–8) new begemotane sesquiterpenoids were separated from *Acer truncatum*-associated *P. brasiliense*. Compounds 5–8 possess 9-oxatricyclo[4.3.0.0^{4,7}]nonane and 4-oxatricyclo[3.3.1.0^{2,7}]nonane skeletons, respectively. Compound 5 is a brasilamide A (1) hydrogenated analog having a tetrahydro-2H-pyrone moiety connected at C-2 and C-5 to a bicyclo[3.1.1]heptane ring to give 4-oxatricyclo[3.3.1.0^{2,7}]nonane skeleton. Brasilamides M (7) and L (6) are oxygenated and hydrogenated derivatives of brasilamide C (3), respectively, while 8 is structurally related to 3, featuring a C-1 methyl group, a C-8 carboxyl carbon, and a C-12 hydroxy

Table 1. Secondary metabolites reported from *P. brasiliense* (chemical class, molecular weight and formulae, fungal source, host, and location).

Chemical class	Compound name	Mol. Wt.	Mol. formula	Strain, host (part, family)	Location	Reference			
Bergamotane sesquiterpenoids	Brasilamide A (1)	293	C ₁₅ H ₁₉ NO ₅	M3–3341, <i>Acer truncatum</i> Bunge (branches, Sapindaceae)	Dongling Mountain, Beijing, China	[25]			
						[26]			
	Brasilamide B (2)	265	C ₁₅ H ₂₃ NO ₃			[25]			
	Brasilamide C (3)	279	C ₁₅ H ₂₁ NO ₄			[25]			
						[26]			
	Brasilamide D (4)	321	C ₁₇ H ₂₃ NO ₅			[25]			
		Brasilamide K (5)	279	C ₁₅ H ₂₁ NO ₄		[26]			
		Brasilamide L (6)	265	C ₁₅ H ₂₃ NO ₃					
		Brasilamide M (7)	293	C ₁₅ H ₁₉ NO ₅					
		Brasilamide N (8)	279	C ₁₅ H ₂₁ NO ₄					
		Brasilterpene A (9)	294	C ₁₆ H ₂₂ O ₅	HDN15-135, Deep-sea sediment	Indian Ocean, China	[27]		
		Brasilterpene B (10)	294	C ₁₆ H ₂₂ O ₅					
		Brasilterpene C (11)	278	C ₁₆ H ₂₂ O ₄					
		Brasilterpene D (12)	278	C ₁₆ H ₂₂ O ₄					
		Brasilterpene E (13)	278	C ₁₆ H ₂₂ O ₄					
	Pinthunamide (14)	277	C ₁₅ H ₁₉ NO ₄	M3–3341, <i>Acer truncatum</i> Bunge (branches, Sapindaceae)	Dongling Mountain, Beijing, China	[25]			
Bisabolane sesquiterpenoids	Brasilamide E (15)	245	C ₁₅ H ₁₉ NO ₂	M3–3341, <i>Acer truncatum</i> Bunge (branches, Sapindaceae)	Dongling Mountain, Beijing, China	[25]			
	Brasilamide F (16)	279	C ₁₅ H ₂₁ NO ₄						
	Brasilamide G (17)	261	C ₁₅ H ₁₉ NO ₃						
	Brasilamide H (18)	261	C ₁₅ H ₁₉ NO ₃						
	Brasilamide I (19)	295	C ₁₅ H ₂₁ NO ₅						
	Brasilamide J (20)	337	C ₁₇ H ₂₃ NO ₆						
	Niduloic acid (21)	276	C ₁₅ H ₁₆ O ₅						
Eremophilane sesquiterpenoids	Paraconiothin A (22)	292	C ₁₇ H ₂₄ O ₄	ECN258, <i>Cinnamomum camphora</i> (L.) J. Presl (healthy twig, Lauraceae)	Nagoya, Japan	[28]			
	Paraconiothin B (23)	308	C ₁₇ H ₂₄ O ₅						
	Paraconiothin C (24)	236	C ₁₅ H ₂₄ O ₂						
	Paraconiothin D (25)	252	C ₁₅ H ₂₄ O ₃						
	Paraconiothin E (26)	252	C ₁₅ H ₂₄ O ₃						
	Paraconiothin F (27)	236	C ₁₅ H ₂₂ O ₂						
	Paraconiothin G (28)	248	C ₁₅ H ₂₀ O ₃						
	Paraconiothin H (29)	246	C ₁₅ H ₁₈ O ₃						
	Paraconiothin I (30)	250	C ₁₅ H ₂₂ O ₃						
	Paraconiothin J (31)	250	C ₁₅ H ₂₂ O ₃						
	Phomadecalin D (32)	264	C ₁₅ H ₂₀ O ₄						
	Phomadecalin E (33)	266	C ₁₅ H ₂₂ O ₄						
	Phomadecalin F (34)	264	C ₁₅ H ₂₀ O ₄						
	8 α -Monoacetoxypomadecalin D (35)	306	C ₁₇ H ₂₂ O ₅						
	Isophomenone (36)	264	C ₁₅ H ₂₀ O ₄						
	(6 <i>S</i> ,8 <i>aS</i>)-6-((<i>S</i>)-1,2-Dihydroxypropan-2-yl)-4,8 <i>a</i> -dimethyl-6,7,8,8 <i>a</i> -tetrahydronaphthalen-1(5 <i>H</i>)-one (37)	250	C ₁₅ H ₂₂ O ₃				MZ-1, <i>Acrida cinerea</i> (healthy insect gut, Acrididae)	Shennongjia Forest District, National Natural Protection Region of China	[16]
	(6 <i>S</i> ,8 <i>aS</i>)-6-((<i>R</i>)-1,2-Dihydroxypropan-2-yl)-4,8 <i>a</i> -dimethyl-6,7,8,8 <i>a</i> -tetrahydronaphthalen-1(5 <i>H</i>)-one (38)	250	C ₁₅ H ₂₂ O ₃						
	(6 <i>S</i> ,8 <i>aS</i>)-4,8 <i>a</i> -Dimethyl-6-(prop-1-en-2-yl)-6,7,8,8 <i>a</i> -tetrahydronaphthalen-1(5 <i>H</i>)-one (39)	216	C ₁₅ H ₂₀ O						

(Continued)

Chemical class	Compound name	Mol. Wt.	Mol. formula	Strain, host (part, family)	Location	Reference
Furanone derivatives	Paraconfuranone A (40)	236	C ₁₄ H ₂₀ O ₃	MZ-1, <i>Acrida cinerea</i> (healthy insect gut, Acrididae)	Shennongjia Forest District, National Natural Protection Region of China	[29]
	Paraconfuranone B (41)	236	C ₁₄ H ₂₀ O ₃			
	Paraconfuranone C (42)	234	C ₁₄ H ₁₈ O ₃			
	Paraconfuranone D (43)	234	C ₁₄ H ₁₈ O ₃			
	Paraconfuranone E (44)	236	C ₁₃ H ₁₆ O ₄			
	Paraconfuranone F (45)	306	C ₁₇ H ₂₂ O ₅			
	Paraconfuranone G (46)	322	C ₁₇ H ₂₂ O ₆			
	Paraconfuranone H (47)	306	C ₁₇ H ₂₂ O ₅			
	Paraconfuranone I (48)	232	C ₁₄ H ₁₆ O ₃			[30]
	Paraconfuranone J (49)	308	C ₁₈ H ₂₈ O ₄			
	Paraconfuranone K (50)	270	C ₁₄ H ₂₂ O ₅			
	Paraconfuranone L (51)	322	C ₁₇ H ₂₂ O ₆			
	Paraconfuranone M (52)	364	C ₁₉ H ₂₄ O ₇			
	6(7)-Dehydro-8-hydroxyterrefuranone (53)	234	C ₁₄ H ₁₈ O ₃			
	8-Hydroxyterrefuranone (54)	252	C ₁₄ H ₂₀ O ₄			
Xanthenes and anthraquinone derivatives	Ethyl 8-Hydroxy-9-oxo-9H-xanthene-1-carboxylate (55)	284	C ₁₆ H ₁₂ O ₅	GY-1, <i>Eucommia ulmoides</i> (stem, Eucommiaceae)	Beichuan County, Sichuan, China	[20]
	Vertexanthone (56)	270	C ₁₅ H ₁₀ O ₅			
	2-Hydroxy-9H-xanthen-9-one (57)	212	C ₁₃ H ₈ O ₃			
	Hydroxyvertexanthone (58)	286	C ₁₅ H ₁₀ O ₆			
	3,4-Dihydroglobosuxanthone A (59)	306	C ₁₅ H ₁₄ O ₇			
	1,8-Dihydroxy-2-(1-hydroxyethyl)anthracene-9,10-dione (60)	284	C ₁₆ H ₁₂ O ₅			
	Chrysazin (61)	240	C ₁₄ H ₈ O ₄			
	Chrysophanol (62)	254	C ₁₅ H ₁₀ O ₄			
Dihydroisocoumarin derivatives	(R)-8-Hydroxy-7-methoxy-3-methylisochroman-1-one (63)	208	C ₁₁ H ₁₂ O ₄	MZ-1, <i>Acrida cinerea</i> (healthy insect gut, Acrididae)	Shennongjia Forest District, National Natural Protection Region of China	[16]
	(R)-7,8-Dimethoxy-3-methylisochroman-1-one (64)	222	C ₁₂ H ₁₄ O ₄			
	(R)-Mellein methyl ether (65)	192	C ₁₁ H ₁₂ O ₃			
	(3R,4R)-cis-4-Hydroxymellein (66)	194	C ₁₀ H ₁₀ O ₄			
	(3R,4S)-cis-4-Hydroxymellein (67)	194	C ₁₀ H ₁₀ O ₄			
	(3S,4S)-cis-4-Hydroxymellein (68)	194	C ₁₀ H ₁₀ O ₄			
	(3S,4R)-cis-4-Hydroxymellein (69)	194	C ₁₀ H ₁₀ O ₄			
	(3S)-cis-7-Hydroxymellein (70)	194	C ₁₀ H ₁₀ O ₄			
Alkaloids and other nitrogenous derivatives	Perlolyrine (71)	264	C ₁₆ H ₁₂ N ₂ O ₂	<i>P. Brasiliense</i> , endophytic fungus	China	[31]
	Flazin (72)	308	C ₁₇ H ₁₂ N ₂ O ₄			
	1-(1',2'-Dideoxy- α -D-nucleopyranosyl)- β -carboline (73)	268	C ₁₆ H ₁₆ N ₂ O ₂			
	Tangutorid E (74)	318	C ₁₆ H ₁₈ N ₂ O ₅			
	1-Acetyl- β -carboline (75)	210	C ₁₃ H ₁₀ N ₂ O			
	4-(9H- β -carbolin-1-yl)-4-oxobutyric acid (76)	268	C ₁₅ H ₁₂ N ₂ O ₃			
	1-(Furan-2-yl)-9H-pyrido[3,4-b]indole (77)	234	C ₁₅ H ₁₀ N ₂ O			
	Indole-3-ethanol (78)	161	C ₁₀ H ₁₁ NO			
	indole-3-acetic acid (79)	175	C ₁₀ H ₉ NO ₂			
	Indole-3-carboxaldehyde (80)	145	C ₉ H ₇ NO			
	2,5- Piperazinedione (81)	114	C ₄ H ₆ N ₂ O ₂	KNUFPCPF01, <i>Capsicum annum</i> L. (healthy bell pepper, Solanaceae)	Local former market, Chuncheon, Korea	[32]

(Continued)

Chemical class	Compound name	Mol. Wt.	Mol. formula	Strain, host (part, family)	Location	Reference
Other metabolites	Dipentene (82)	136	C ₁₀ H ₁₆	KNUFCPF01, <i>Capsicum annum</i> L. (healthy bell pepper, Solanaceae)	Local former market, Chuncheon, Korea	[32]
	O-Cymene (83)	134	C ₁₀ H ₁₄			
	4-Carvomenthenol (84)	154	C ₁₀ H ₁₈ O			
	γ-Terpinene (85)	136	C ₁₀ H ₁₆			
	2-Phenylethanol (86)	122	C ₈ H ₁₀ O			
	2-Phenethyl acetate (87)	164	C ₁₀ H ₁₂ O ₂			
	2,4-Di-tertbutylphenol (88)	206	C ₁₄ H ₂₂ O			
	3,5-Nonadien-7-yn-2-ol (89)	136	C ₉ H ₁₂ O			
	2,3-Butylene glycol (90)	90	C ₄ H ₁₀ O ₂			
	Isopentyl acetate (91)	130	C ₇ H ₁₄ O ₂			
	Heneicosane (92)	296	C ₂₁ H ₄₄			

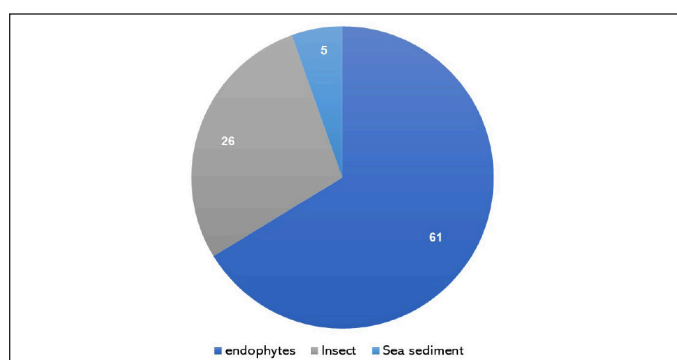


Figure 1. Number of metabolites reported from *P. brasiliense* separated from various sources.

group in **8** instead of oxymethylene, methylene, and a ketone carbonyl, respectively, in **3**. The 12*S* configuration in **8** was assigned by the modified Mosher method [26]. In addition, **9–13** with unusual spiral 6/4/5 tricyclic ring skeleton were separated from the deep sea-derived HDN15-135 strain by RP-18/SiO₂/Sephadex LH-20 column chromatography (CC)/HPLC that were elucidated using NMR/X-ray/electronic circular dichroism (ECD)/density-functional theory calculations [27].

Bisabolane sesquiterpenoids

In 2015, Liu *et al.* separated new bisabolane sesquiterpenoids: **15–20**, having 3-cyclohexylfuran (**15** and **16**) and 3-cyclohexylfuranone (**17–20**) frameworks in addition to the known analog **21** possesses 3-cyclohexylfuranone skeleton from *P. brasiliense* culture EtOAc extract by SiO₂/Sephadex LH-20 CC/reversed phase-High-performance liquid chromatography (RP-HPLC). Compounds **17–20** were obtained as racemic, where **17** and **18** were separated by a chiral HPLC column (Fig. 3). The configurations of **17** and **18** were assigned by ECD calculations [33].

Eremophilane sesquiterpenoids and octahydronaphthalene derivatives

New sesquiterpenoids: paraconiothins A–J (**22–31**), together with **32–36** were purified from *Cinnamomum*

camphora-associated *P. brasiliense* ECN-258 EtOAc fraction using SiO₂/Sephadex LH-20 CC (Fig. 4). Compounds **22–28** are eremophilane derivatives, while **29–31** are proposed to be biosynthesized from the eremophilane-sesquiterpenoid skeleton rearrangement. Compounds **22** and **23** possess a C-7 β-configured isopropyl-like substituent opposite to that in **24–27** with a C-6/C-7 epoxy group [28]. The biosynthesis of **29–31** was speculated to involve Wagner-Meerwein-type rearrangement and aromatization of eremophilanes (Scheme 1). Their carbocation intermediates are formed by the loss of a C-8 group. Paraconiothin H (**29**) is generated by aromatization with a proton loss following a 1,2-methyl shift from C5 to C6. While paraconiothins I (**30**) and J (**31**) could be formed through the spiro-carbocation produced by a 1,2-alkyl shift from C₅ to C₁₀ [28].

Recently, Li *et al.* separated from *P. brasiliense* EtOAc extract, new octahydronaphthalene derivatives: **37–39** that were elucidated by NMR, high resolution mass spectrometry (HRMS), ECD/CD, and X-ray analyses [16]. Their configurations were assigned as 7*S*/10*S*/11*S*, 7*S*/10*S*/11*R*, and 7*S*/10*S*, respectively [16].

Furanone derivatives

Furanones are oxygenated heterocyclic metabolites that have been separated from different natural origins, including fungi of certain genera such as *Cephalosporium*, *Aspergillus*, and *Paraconiothyrium* [30]. From the gut of *Acrida cinerea* insect isolated Protein Data Bank (PDB) culture of *P. brasiliense* MZ-1 collected from Shennongjia Forest District, new furanone derivatives: **40–47** were isolated and characterized using SiO₂/RP-HPLC and NMR data, respectively [29]. Their 5*R* configuration was assigned based on CD analysis (Fig. 5). They were proposed to be biosynthesized from malonyl CoA and acetyl CoA (Scheme 2).

In another study in 2016, Liu *et al.* further reported new furanones, paraconfuranones I–M (**48–52**), along with **53** and **54** from the same strain MZ-1 cultured on malt extract (ME) medium [30]. From these two studies, it was noted that the profile of the produced metabolites varied according to the type of culture media.

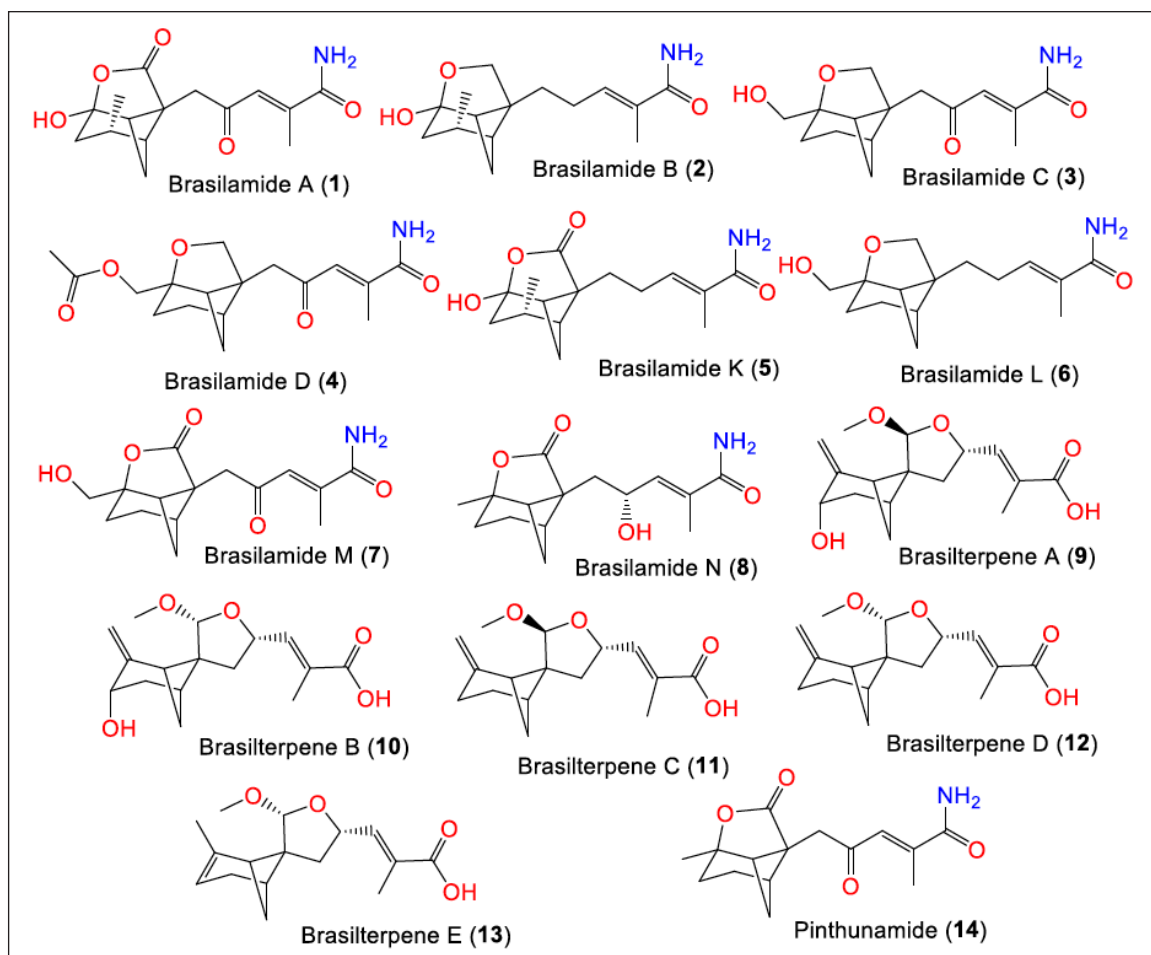


Figure 2. Structures bergamotane sesquiterpenoids (1–14) reported from *P. brasiliense*.

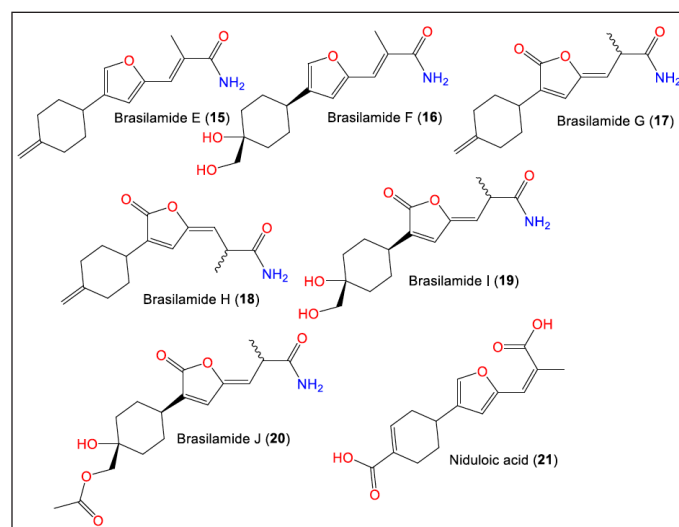


Figure 3. Structures of bisabolane sesquiterpenoids (15–21) reported from *P. brasiliense*.

Anthraquinone and xanthone derivatives

Xu *et al.* purified a new xanthone and anthraquinone derivatives: **55** and **60**, respectively, along with known analogs:

56–62 from the EtOAc extract of *P. brasiliense* GY-1 culture isolated from *Eucommia ulmoides* stem, collected in Beichuan County/Sichuan Province/China using SiO₂/Sephadex LH-20/HPLC (Fig. 6) [20].

Alkaloids and iso-coumarin derivatives

Li *et al.* purified and characterized new dihydroisocoumarins; **63**, and **64**, along with **65–70** that were elucidated by NMR, HRMS, ECD/CD, and X-ray analyses (Fig. 7) [16]. Their configurations were assigned as 7S/10S/11S, 7S/10S/11R, and 7S/10S, respectively [16]. In 2021, Zhou *et al.* purified and characterized for the first-time indole and β -carboline alkaloids [31] (Fig. 8).

Other constituents

Furthermore, gas chromatography mass spectrometry analysis revealed that **82–85** are among the 12 major constituents detected in the EtOAc extract of *P. brasiliense* obtained from *Capsicum annuum* fruit (Fig. 9) [32]. These compounds had significant molecular interaction with dihydropteroate synthase in the molecular docking examination. Dihydropteroate synthase inhibition is one of the targets to inhibit or kill bacteria via pterin-sulfonamide conjugation [32]. In addition, the extract was found to contain phenolics (2.59 mg/g gallic acid

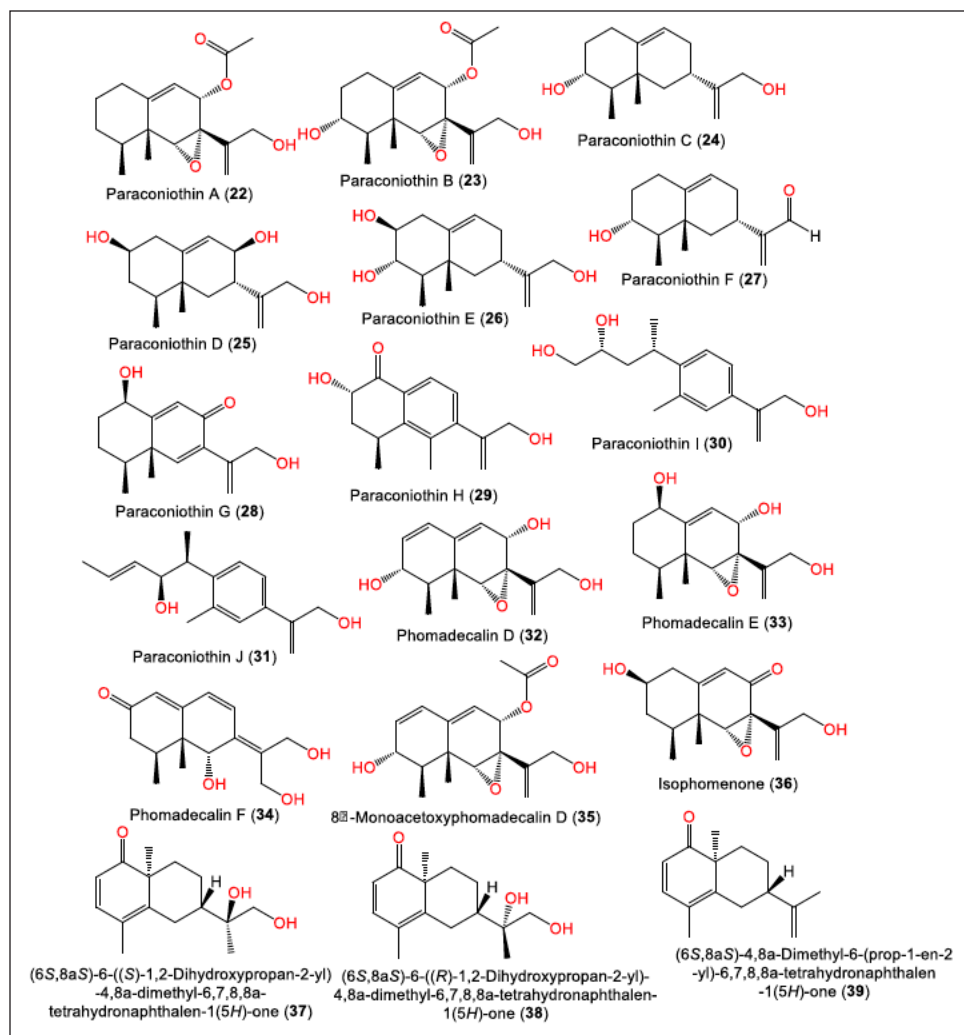
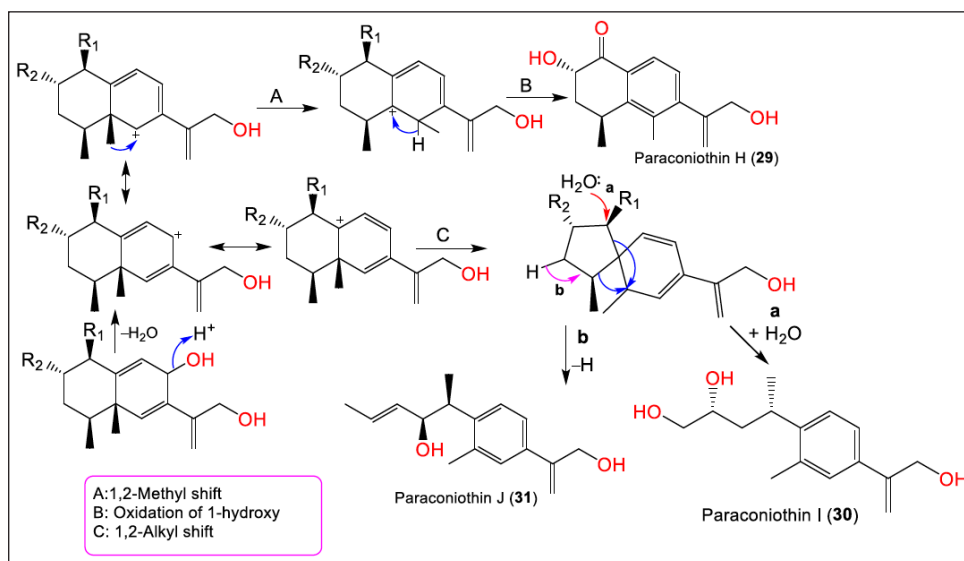


Figure 4. Structures of eremophilane sesquiterpenoids (22–36) and octahydronaphthalene derivatives (37–39) reported from *P. brasiliense*.



Scheme 1. Biosynthetic pathway of 29–31 [28].

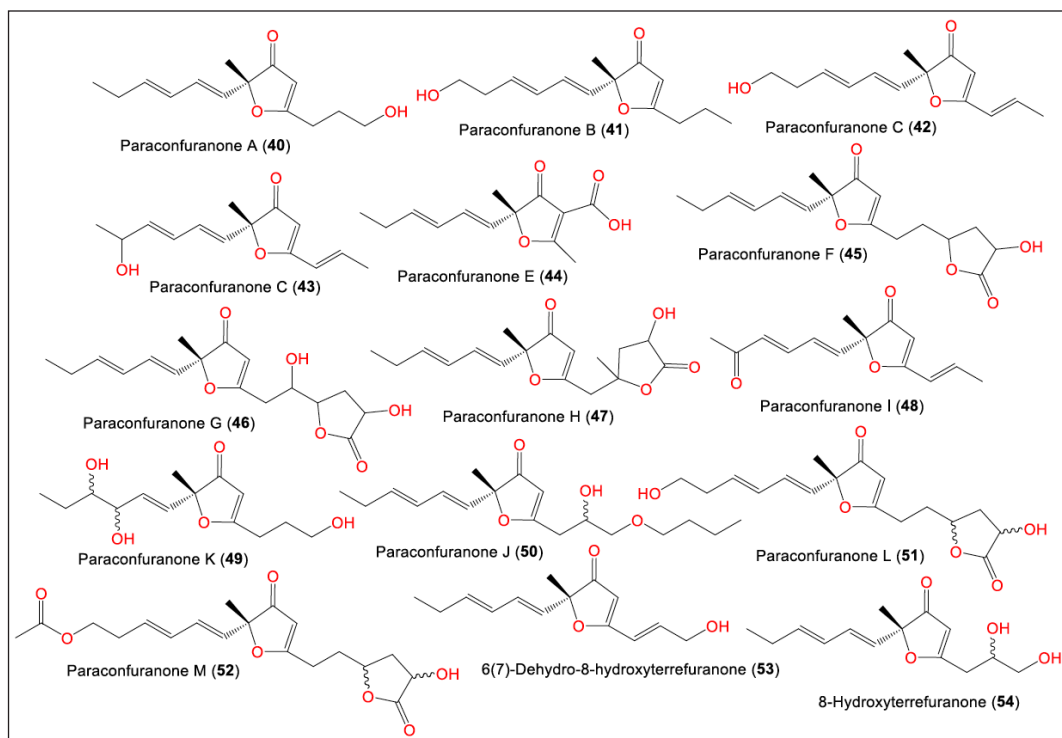
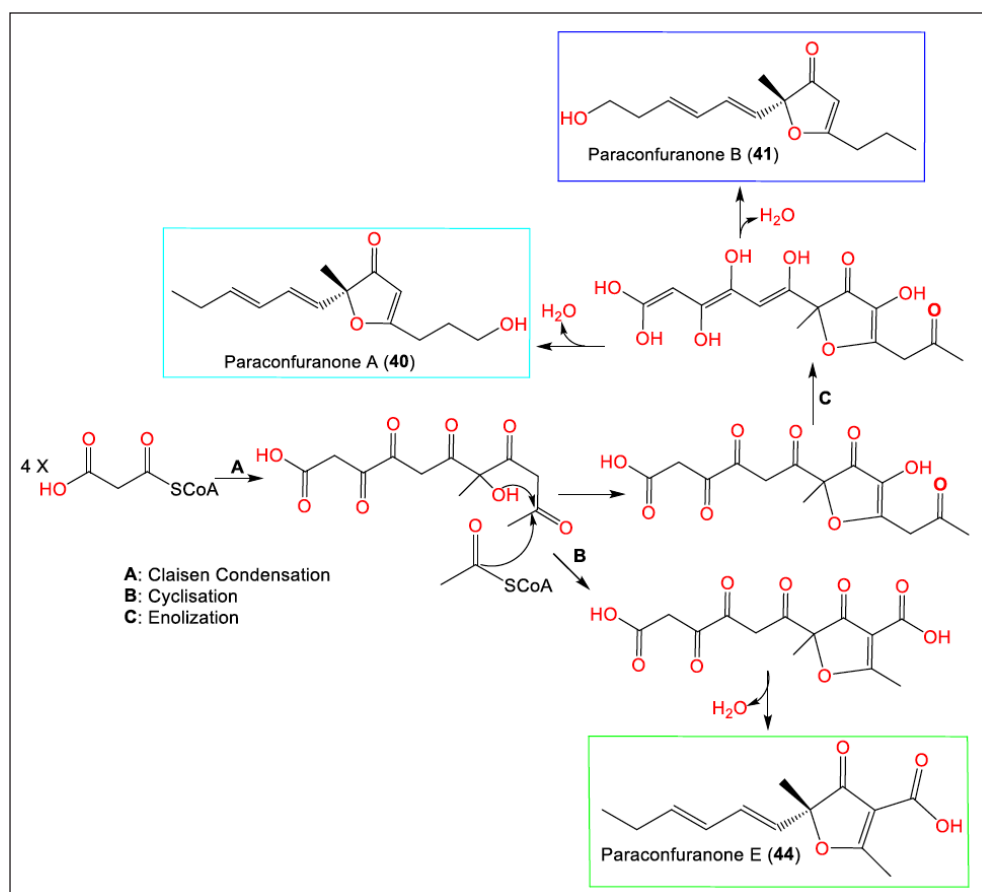


Figure 5. Structures of furanones (40–54) reported from *P. brasiliense*.



Scheme 2. Biosynthetic pathway of 40, 41, and 44 from malonyl CoA and acetyl CoA [29].

equivalent of extract) and flavonoids (31.53 mg/g quercetin equivalent of extract) [32].

BIOACTIVITIES OF *P. BRASILINSE* METABOLITES

Although a considerable number of secondary metabolites were reported from *P. brasiliense*, limited studies have assessed the bioactivities of these metabolites. In addition, most of these investigations have been carried

out *in vitro* without exploring the possible mechanisms of action of these compounds. These studies have been highlighted below.

Antiviral and anti-platelet aggregation activities

In 2010, Liu *et al.* reported that **2–4** (Half maximal effective concentrations (EC_{50}) 108.8, 57.4, and 48.3 μ M, respectively) demonstrated inhibition capacity on the

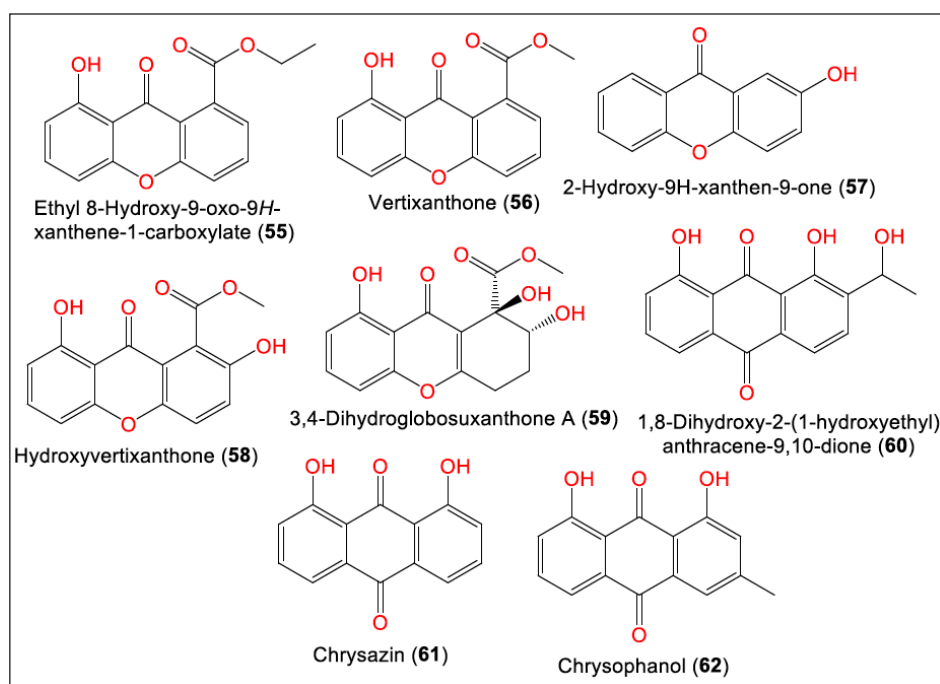


Figure 6. Structures of xanthenes (55–59) and anthraquinones (60–62) reported from *P. brasiliense*.

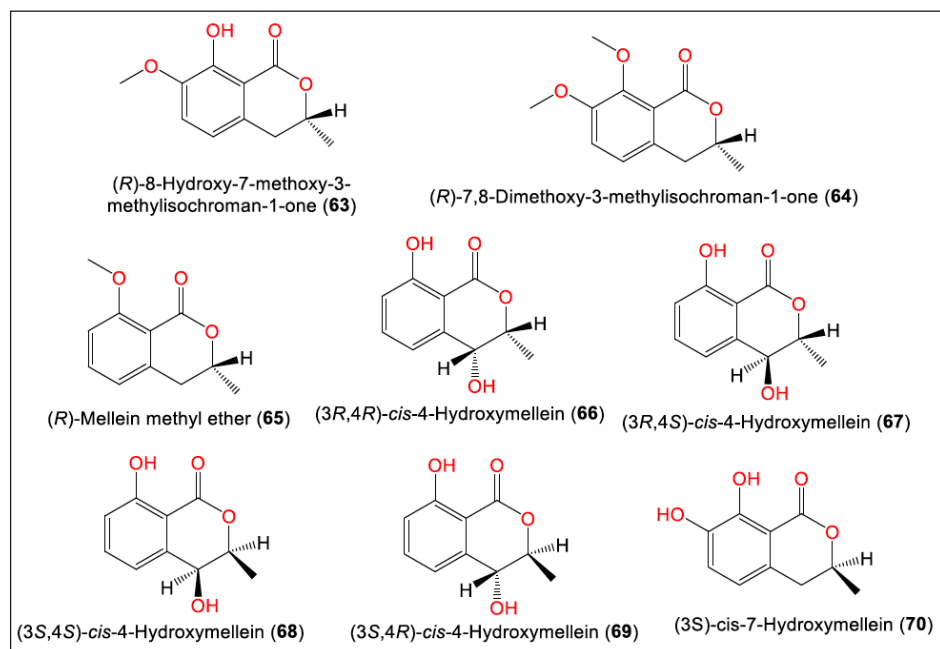


Figure 7. Structures of dihydroisocoumarins (63–70) reported from *P. brasiliense*.

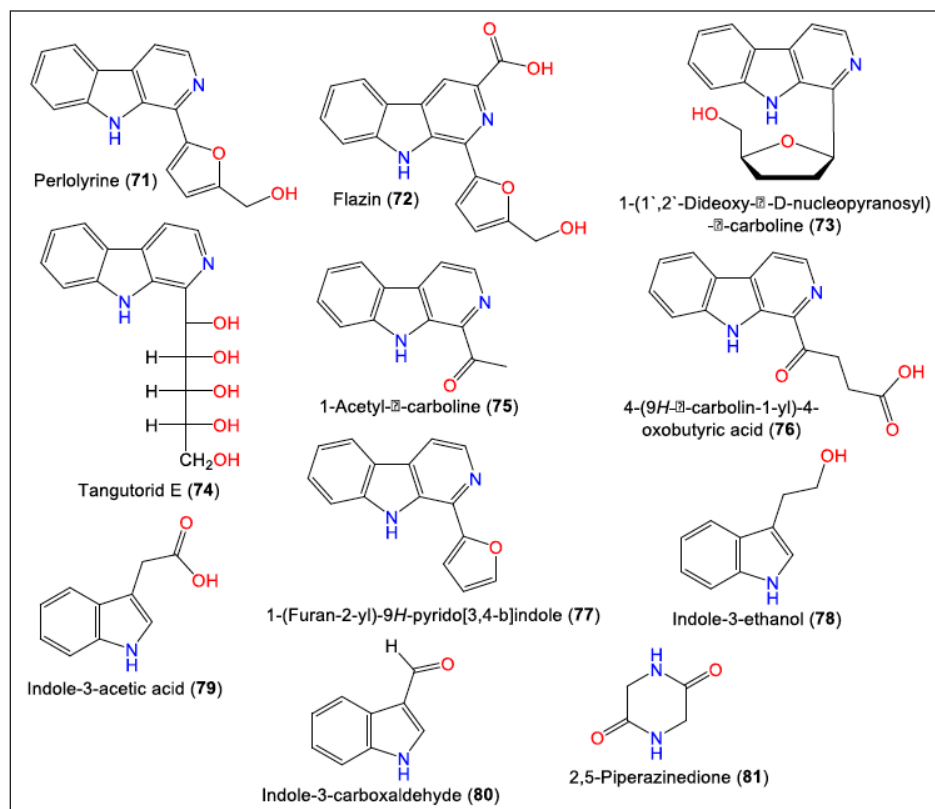


Figure 8. Structures of alkaloids (71–81) reported from *P. brasiliense*.

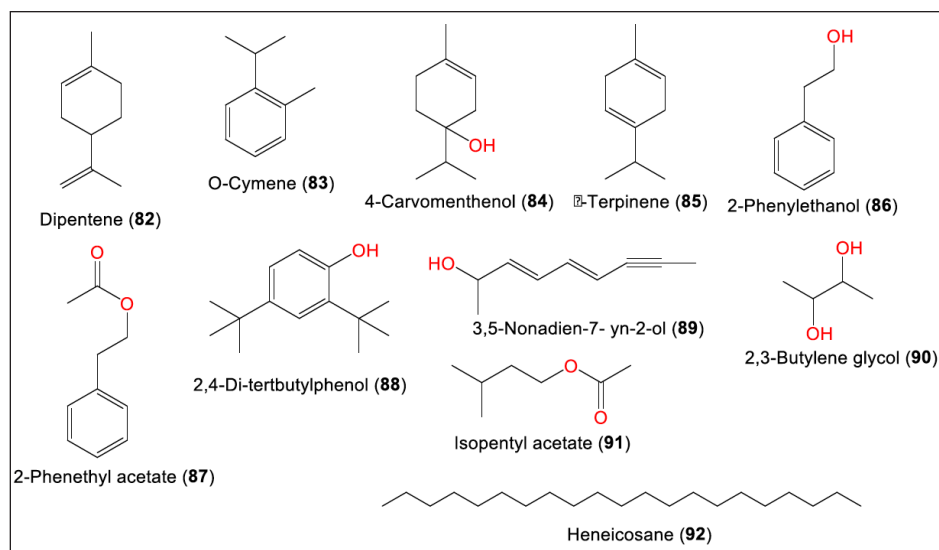


Figure 9. Other metabolites (82–92) reported from *P. brasiliense*.

replication of HIV-1 in human T cell leukaemia cells, compared to indinavir sulfate (EC_{50} 8.2 nM) [25]. In addition, **37–39** (Conc. 1 mmol/L) possessed platelet aggregation inhibitory potential (%inhibition 0.70%–15.91%) [16], whereas **39** had the better inhibitory capacity (inhibition 15.91%) compared to aspirin (%inhibition 14.73%) [16]. Compounds **63**, **64**, and **66–69** (Conc. 1 mmol/L) possessed platelet aggregation inhibitory potential [16].

Cytotoxic activity

Unfortunately, compounds **5–8** (Conc. 50 μ M) had no notable cytotoxicity against human lung adenocarcinoma cells (A549), human malignant melanoma cells, human breast adenocarcinoma cell line (MCF-7) (human breast cancer cells), stable oncoprotein latent membrane protein 1 integrated nasopharyngeal carcinoma cells, human esophageal cancer cells, human gastric cancer cells (MGC),

human pancreatic carcinoma cells, and human hepatoma carcinoma cells [26].

In 2016, Zhang *et al.* semi-synthesized 27 derivatives from brasilamide E (**15**) to improve its cytotoxic efficacy. Compound **15** specifically inhibited the proliferation of MCF-7 and human ovarian cancer cell line (HO8910) (human ovarian) cell lines (half-maximal inhibitory concentration (IC_{50}) 8.47 and 18.0 μ M, respectively) and had no effect on human keratinocyte cell line and mouse embryonic fibroblast cells (NIH3T3) cells ($IC_{50} > 50$ μ M). In the semisynthetic derivatives, it was noted that methylene cyclohexane ring replacement in **15** with substituted phenyl rings retained selectivity and increased activity. In addition, ring B substitution patterns and substituents influenced the selectivity, whereas electron-withdrawing groups on the phenyl ring were essential for maintaining the selectivity [34].

The cytotoxic assessment of **15–20** revealed that **15** (IC_{50} 8.4 μ M) was active versus MCF-7 cells and inhibited the MGC cells proliferation (IC_{50} 14.7 μ M), compared to paclitaxel (IC_{50} 6.4 nM) in the (3-(4,5-Dimethylthiazol-2-yl)-5-(3-carboxymethoxyphenyl)-2-(4-sulfophenyl)-2H-tetrazolium inner salt) assay, while **16–20** had no effects. Compound **15** specifically impaired MCF-7 glucose metabolism by tumor cells, without affecting the normal cells. Compound **15** induced its inhibitory effectiveness on MCF-7 cells through inhibition of lactate secretion, glucose consumption, and adenosine triphosphate generation [33]. These compounds **40–47** had no cytotoxic potential on A549, HepG 2, and Caski in the 3-(4,5-Dimethylthiazol-2-yl)-2,5-diphenyltetrazolium bromide (MTT) assay [29].

Neuroprotective and xanthine oxidase inhibitory activities

Liu *et al.* *in vitro* assessed **48**, **50**, **51** **53**, and **54** for their neuroprotective capacity versus hydrogen peroxide-induced damage in rat adrenal pheochromocytoma cell line cells. It was found that **48** (Conc. 12.5 μ g/ml) demonstrated powerful *in vitro* neuroprotective potential similar to that of edaravone, indicating its possible use as a lead for developing drugs treating CNS disorders [30].

It is noteworthy that **71–80** showed obvious xanthine oxidase inhibition potential activity inhibitory activity (IC_{50} s from 0.68 to 9.30 μ M). It was noted that **73**, **72**, and **76** displayed better activity than standard drugs [31].

Hypoglycemic and anti-hypercholesteremic activities

In 2022, Wang *et al.* reported that **9** and **11** (Conc. 10 μ M) remarkably lessened the glucose levels to 449.3 and 420.4 pmol/larva, respectively, after incubating with β -cell ablated zebrafish larvae without any toxicity up to Conc. 200 μ M. Their hypoglycemic effectiveness was attributed to suppressing gluconeogenesis and improving insulin sensitivity rather than inducing β -cells regeneration. The structure-activity relation study demonstrated that the endocyclic double bond, C-14S configuration, and lack of C-3-OH boosted the activity. On the other hand, **9–13** did not affect the β -cell number [22].

The effect of **22–26** and **28–36** was tested on nuclear receptors, namely, Liver X receptor-alpha (LXR α),

the peroxisome proliferator-activated receptors γ and δ , and the retinoic acid receptor α . Compounds **24** and **30** exhibited a significant inhibition effect for LXR α (Conc. 50 μ M), while **24** and **30** (Conc. 50 μ M) had no cytotoxicity versus human embryonic kidney cell line cells in the luciferase reporter gene and MTT assay, respectively. LXR regulates the expression of genes involved in the transport, excretion, and catabolism of cholesterol. LXR activation promotes lipogenesis via up-regulating lipogenic enzyme genes such as sterol-regulatory element-binding transcription factor-1 (Srebf1) and fatty acid synthase, LXR antagonists could be beneficial in treating nonalcoholic fatty liver disorder [28].

Bioactivities of *P. brasiliense* extract

Sathiyaseelan *et al.* reported that the EtOAc extract possessed notable antioxidant potential by scavenging 1, 1-Diphenyl-2-picrylhydrazyl, 2,2'-Azinobis-(3-ethylbenzthiazoline-6-sulphonate, and Fe³⁺ radicals with (IC_{50} s 383.51, 29.57, and 358 μ g/ml, respectively) compared to ascorbic acid (IC_{50} s 69.11, 41.84, and 317.6 μ g/ml, respectively) [32]. It also had marked cytotoxic capacity on PC3 cells (IC_{50} 187.3 μ g/ml), but it had less activity versus HEK-293 cells in the water-soluble tetrazolium salt viability assay and no inhibition activity on α -amylase and α -glucosidase. It demonstrated antibacterial potential versus *Bacillus cereus*, *Staphylococcus aureus*, *Listeria monocytogens*, *Escherichia coli*, and *Salmonella enterica* (inhibition zone diameters (IZDs) 8.0–24.0 mm, and minimum inhibitory concentrations (MICs) 15.62–62.5 μ g/ml), compared to tetracycline hydrochloride (IZDs 12.0–23.0 mm) [32]. It possessed antagonistic efficacy versus *Phytophthora* sp. and *Colletotrichum* sp. [19]

Applications of *P. brasiliense*

Sathiyaseelan *et al.* synthesized and characterized titanium dioxide nanoparticles (TiO₂NPs) using *P. brasiliense* aqueous extract. The antibacterial assay revealed that *P. brasiliense*-TiO₂ nanoparticles (NPs) (20 μ g/ml) had no notable antibacterial activity while its combination with tetracycline hydrochloride remarkably increased the *E. coli* biofilm inhibition. Furthermore, *P. brasiliense*-TiO₂ nanoparticles (NPs) were moderately toxic versus red blood corpuscle, NIH3T3, and egg embryos. Thus, these NPs can be mixed with antibiotics to enhance antibacterial capacity thereby reducing environmental toxicity and microbial resistance [35].

In 2014, Garyali *et al.* reported that *P. brasiliense* isolated from the stem bark of Himalayan yew (*Taxus baccata* L. ssp. *wallichiana* (Zucc.) Pilger) produced taxol. In addition, it possessed the key genes (C-13 Phenylpropanoid side chain CoA acyltransferase and 10-Deacetylbaaccatin III-10-O-acetyl transferase) that are implicated in taxol biosynthesis [36].

In the plant cell culture, the induction method using fungi was reported to be an efficient technique in enhancing the production of various secondary metabolites [37]. Salehi *et al.* reported that the addition of *P. brasiliense* cell extract and culture filtrate induced paclitaxel production in *Corylus avellana* cell suspension culture, which could be substantial for large-scale and stable production of taxol [38].

Paraconiothyrium brasiliense isolated from *Pachysandra terminalis* was found to exhibit better growth on oatmeal agar than on Potato dextrose agar and malt extract agar [39]. It also revealed the capability for producing extracellular enzymes such as avicelase, amyase, β -glucosidase, xylanase, and protease [39].

Paraconiothyrium brasiliense efficiently assimilated glycogen and dextrin, indicating a good amylolytic enzyme production capacity. In addition, it decolorized Remazol-brilliant blue R, blue 71, and Chicago sky blue dyes. Its extracellular laccase activity reached the maximum (46.8 U/L) in Cu^{2+} -supplemented PDB medium [19]. This could have potential in extracellular laccase production and environmental detoxification [19].

IN SILICO INSIGHTS OF *P. BRASILIENSE* METABOLITES

To further expand understanding of *P. brasiliense* metabolites beyond their known properties, delving into *in silico* studies that elucidate the mechanisms underlying their neuroprotective attributes. Molecular docking was employed to confirm the neuroprotective ability of paraconfuranone compounds and their fit within the binding pocket of KEAP1. In addition, molecular docking suggests novel applications for antibacterial inhibitors, with a specific focus on combatting *Pseudomonas aeruginosa*.

Paraconfuranones neuroprotective activity

According to the displayed data in Table 2, the co-crystallized reference compound (PDB ID: 7OFE) exhibited the highest docking score among the tested compounds, which was -6.633 kcal/mol. Fortunately, Paraconfuranone L (51), Paraconfuranone I (48), and Paraconfuranone J (50) showed similar docking scores to the exciting reference, with scores of -6.612 , -6.305 , and -6.158 kcal/mol, respectively. Although paraconfuranone F (45) and paraconfuranone K (49) had slightly lower docking scores compared to the reference (-5.629 and -5.137 kcal/mol, respectively), they still demonstrated competitive binding. Paraconfuranone M (52) showed a low affinity for KEAP1 with a docking score of -3.817 kcal/mol.

Table 2. Docking scores of the top compounds bound to KEPA1.

Compound	Docking score (kcal/mol)
Reference	-6.633
Paraconfuranone L (51)	-6.612
Paraconfuranone I (48)	-6.305
Paraconfuranone J (50)	-6.158
Paraconfuranone F (45)	-5.629
Paraconfuranone K (49)	-5.137
Paraconfuranone M (52)	-3.817

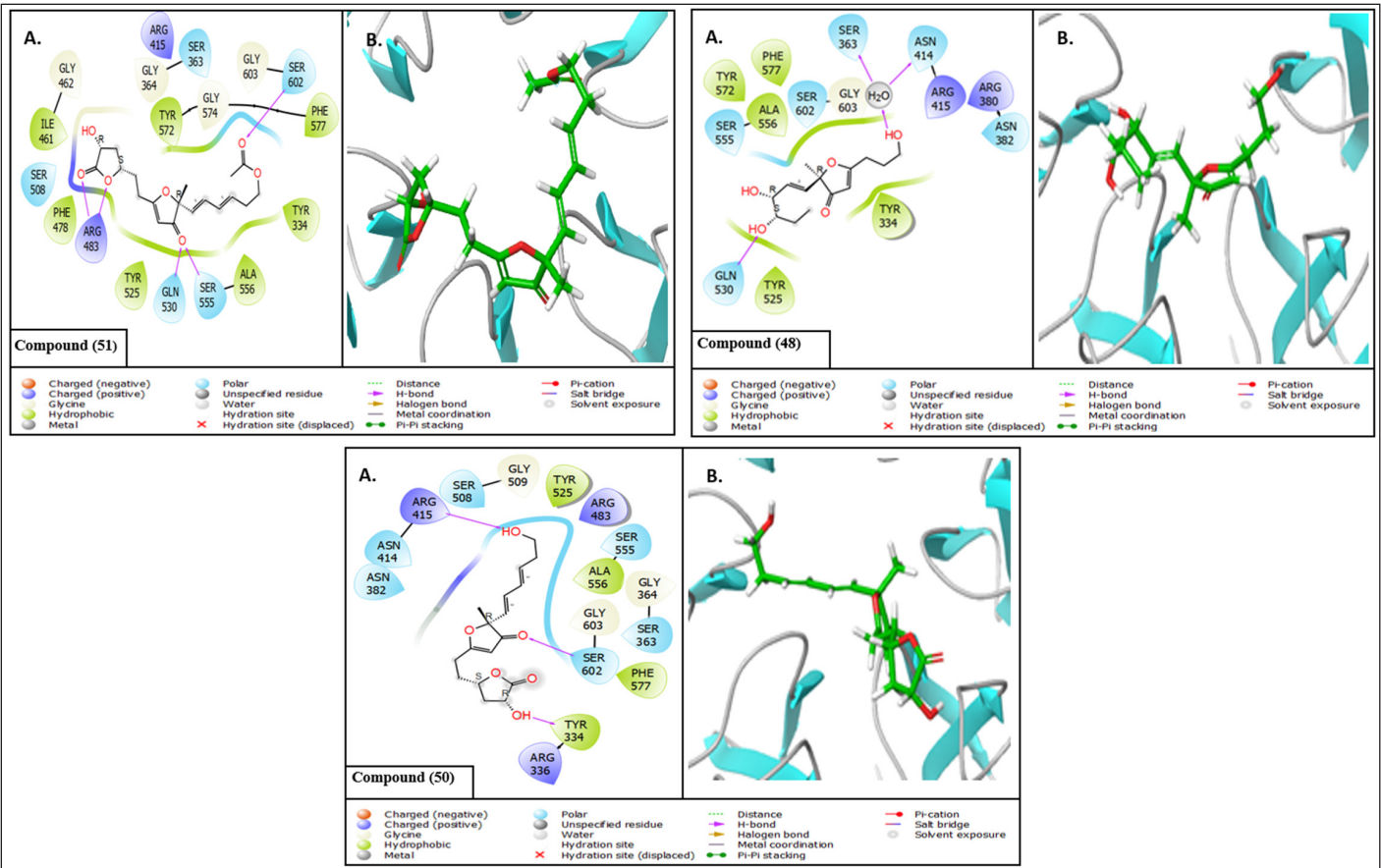


Figure 10. (A) 2D interaction diagrams and (B) 3D interaction diagrams of the top compounds bound to KEAP1.

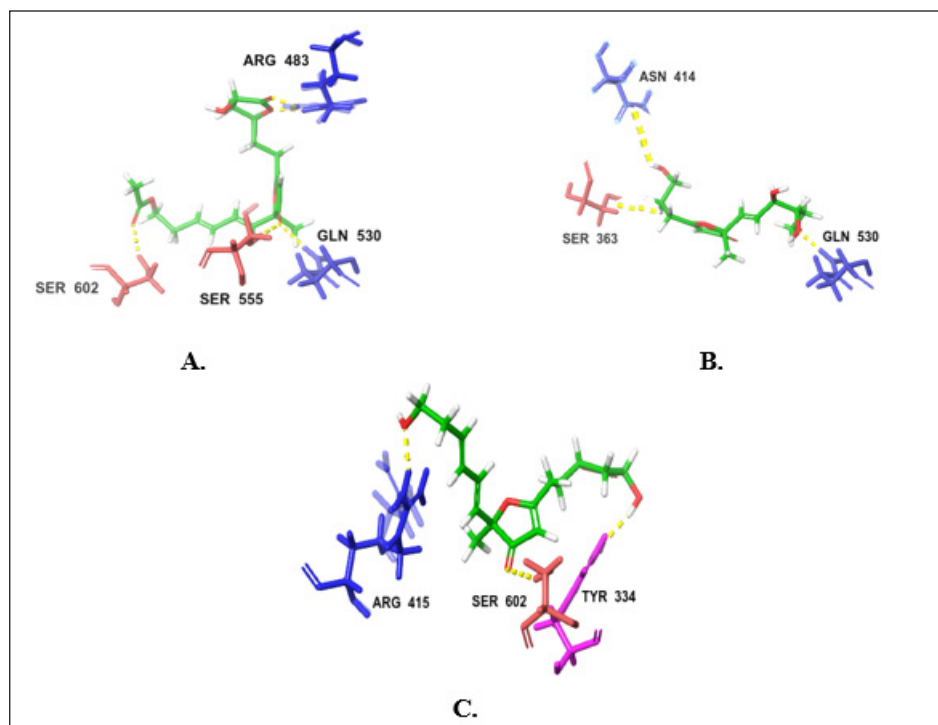


Figure 11. H-bond interactions of the top two compounds with KEPA1. (A) Compound **51**. (B) Compound **48**. (C) compound **50**.

Table 3. Docking scores and molecular interactions of the top brasilamide and paraconifuranone compounds and the reference bound to LasR.

Compound	Docking score (kcal/mol)	HB	Hydrophobic
1-(1',2'-Dideoxy- α -D-nucleopyranosyl)- β -carboline (73)	-11.327	ASP73, SER129	LEU36, LEU39, LEU40, TYR47, ALA50, ILE52, TYR56, TRP60, TYR64, CYS79, VAL76, TRP88, ALA105, PHE101, LEU110, LEU125, ALA127
1-Acetyl- β -carboline (75)	-10.055	ARG61, ASP73, TYR56, SER129	LEU36, LEU40, TYR47, ALA50, ILE52, TYR56, TRP60, TYR64, ALA70, CYS79, VAL76, TRP88, ALA105, PHE101, LEU110, LEU125, ALA127
Reference	-10.023	LEU125, TRP60	LEU36, LEU40, TYR47, ALA50, ILE52, TYR56, TRP60, TYR64, ALA70, VAL76, TRP88, ALA105, PHE101, LEU110, LEU125, ALA127
Brasilamide J (20)	-9.813	SER129, ASP73	LEU39, LEU40, TYR47, ALA50, ILE52, TYR56, TRP60, TYR64, ALA70, VAL76, TRP88, PHE101, LEU125, ALA127
Brasilamide E (15)	-9.576	TYR75	LEU36, LEU40, TYR47, ALA50, ILE52, TYR56, TRP60, TYR64, ALA70, CYS79, VAL76, TRP88, PHE101, LEU125, ALA127
Hydroxyvertixanthone (58)	-9.426	LEU125, TRP60	LEU36, LEU40, TYR47, ALA50, ILE52, TYR56, TRP60, TYR64, ALA70, VAL76, TRP88, ALA105, PHE101, LEU110, LEU125, ALA127
Brasilamide H (18)	-9.39	TYR56, SER129	LEU36, LEU39, LEU40, TYR47, ALA50, TYR56, TRP60, TYR64, ALA70, CYS79, VAL76, TRP88, ALA105, PHE101, LEU110, LEU125, ALA127
Brasilamide B (2)	-9.37	TYR56, SER129	LEU36, LEU39, TYR47, ALA50, TYR56, TRP60, TYR64, ALA70, CYS79, VAL76, TRP88, ALA105, PHE101, LEU110, LEU125, ALA127
Brasilamide I (19)	-9.342	TYR93	LEU36, LEU40, TYR47, ILE52, TYR56, TRP60, TYR64, ALA70, CYS79, VAL76, TRP88, TYR93, ALA105, PHE101, LEU110, LEU125, ALA127
Paraconifuranone J (50)	-9.312	TYR93	LEU36, LEU39, LEU40, TYR47, ALA50, TYR64, ALA70, VAL76, TRP88, ILE92, ALA105, PHE101, LEU110, LEU125, ALA127
Paraconiothion C (24)	-9.813	SER129, THR75	LEU36, LEU40, TYR47, ILE52, TYR56, TRP60, TYR64, ALA70, CYS79, VAL76, TRP88, PHE101, PHE102, LEU125, ALA127

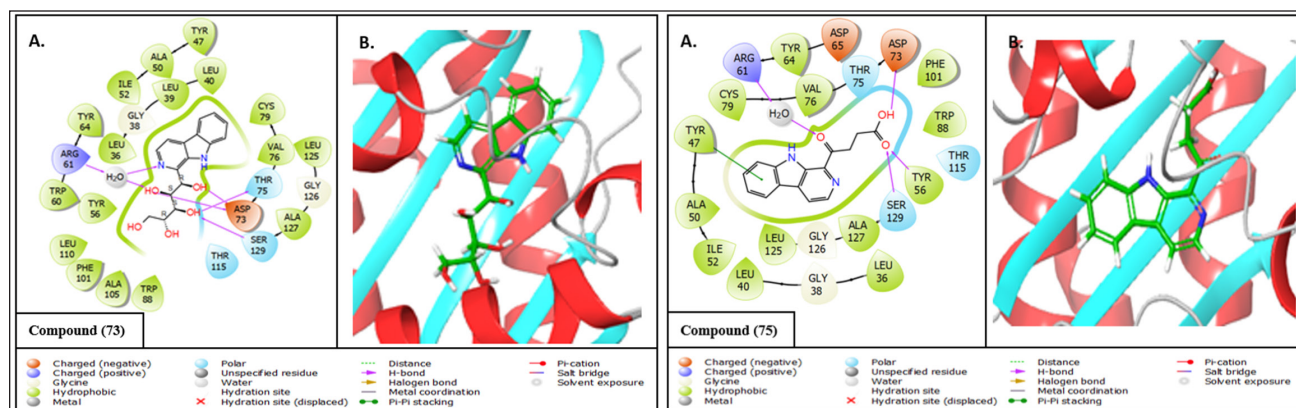


Figure 12. (A) 2D interaction diagrams and (B) 3D interaction diagrams of the top Brasilamide and Paraconifuranone compounds and the reference bound to LasR.

The intermolecular interaction patterns of the Paraconifuranone compounds with docking scores similar to the exciting reference were determined using Schrödinger's ligand interaction diagram, which displays hydrogen bonds, pi-pi stacking, salt bridges, and other intermolecular interactions. Hydrogen bonds play a crucial role in stabilizing the protein-ligand complex. For the KEAP1 protein, compound 1 formed hydrogen bonds with SER602, SER555, GLN530, and ARG483 at distances of 2.04, 1.83, 2.05, and 1.97 Å, respectively. Paraconifuranone L (**51**) also established hydrophobic bonds with TYR572, PHE577, TYR334, ALA556, TYR525, PHE478, and ILE461. Paraconifuranone I (**48**) formed hydrogen bonds with SER363 (1.72 Å), ASN414 (1.72 Å), and GLN530 (1.8 Å), as well as hydrophobic bonds with PHE577, ALA556, TYR525, TYR334, TYR525, and TYR334. Paraconifuranone I (**50**) exhibited hydrogen bonding with ARG415, TYR334, and SER602 at distances of 1.95, 1.95, and 2.16 Å, respectively. It also showed hydrophobic bonds with PHE577, ALA556, TYR525, and TYR334 (Figs. 10 and 11). The reference compound demonstrated hydrogen bond interactions with SER555 and GLN530, as well as hydrophobic interactions with TYR525, ALA556, TYR334, PHE577, and TYR572, which are closely related to our findings.

Brasilamides and paraconifuranones antibacterial activity

For activity against *P. aeruginosa*, molecular docking results of Brasilamide and Paraconifuranone compounds with the LasR protein (PDB ID: 2UV0), indicated that 1-(1',2'-Dideoxy- α -D-nucleopyranosyl)- β -carboline (**73**) exhibited the highest docking score of -11.327 kcal/mol, followed by 1-Acetyl- β -carboline (**75**) with a docking score of -10.055 kcal/mol (Table 3). The reference compound had a docking score of -10.023 kcal/mol, and ten compounds closely followed with competitive docking scores ranging from -9.813 to -9.312 kcal/mol.

The intermolecular interaction patterns of these compounds with LasR were determined using Schrödinger's ligand interaction diagram, as shown in Table 3. Compound (**73**) formed hydrogen bonds with ASP73 at a distance of 1.95 Å and SER129 at a distance of 2.20 Å. It also exhibited hydrophobic interactions with LEU36, LEU39, LEU40, TYR47, ALA50, ILE52, TYR56, TRP60, TYR64, CYS79, VAL76, TRP88,

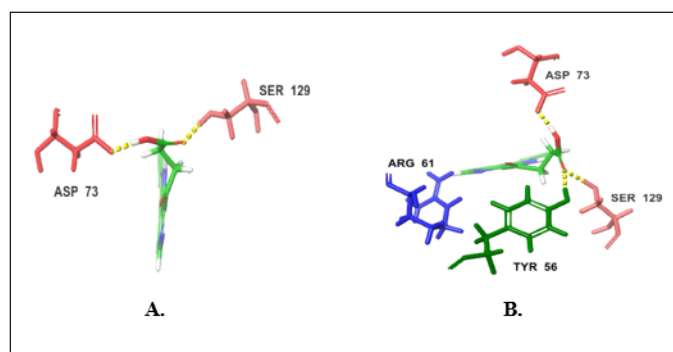


Figure 13. H-bond interactions of the top two compounds with LasR. (A) Compound 73. (B) Compound 75.

ALA105, PHE101, LEU110, LEU125, and ALA127 residues. 1-Acetyl- β -carboline (**75**) formed four hydrogen bonds with ARG61 at a distance of 2.12 Å, ASP73 at a distance of 1.70 Å, TYR56 at a distance of 1.73 Å, and SER129 at a distance of 1.95 Å. In addition, it exhibited hydrophobic interactions with LEU36, LEU40, TYR47, ALA50, ILE52, TYR56, TRP60, TYR64, ALA70, CYS79, VAL76, TRP88, ALA105, PHE101, LEU110, LEU125, and ALA127 residues (Figs. 12 and 13). The interactions of the remaining compounds can be found in Table 3. The reference compound shared hydrophobic interactions with all the compounds.

ABSORPTION, DISTRIBUTION, METABOLISM, EXCRETION, AND TOXICITY (ADMET)

Based on the ADMET prediction using Qikprop and ProTox-II, the top three compounds with similar docking scores to the reference in KEAP1 docking, as well as the top two scoring compounds and the reference in LasR docking, were evaluated. As shown in Table 4, these compounds have Mwt ranging from 270 to 364. The number of donor hydrogen bonds falls within the range of 1 to 4, while the number of acceptable hydrogen bonds ranges from 4 to 9.

The oil/water coefficient (QPlogPo/w) of these compounds is in the range of 0.05 to 2.797. These values satisfy the rule of five, which sets limits for drug likeness. The rule of

Table 4. Lipinski rule parameters for the selected compounds and the references.

Compound	Mol. Wt.	donorHB	acceptHB	QPlogPo/w	Number of rule of five violations
Paraconfurane L (51)	364.394	1	9	1.73	0
Paraconfurane I (48)	270.325	3	7	0.607	0
Paraconfurane J (50)	322.357	2	9	0.962	0
1-(1',2'-Dideoxy- α -D-nucleopyranosyl)- β -carboline (73)	318.329	4	9.5	0.051	0
1-Acetyl- β -carboline (75)	268.271	1	4	2.797	0
LasR Reference	297.394	0	6.5	1.747	0
KEAP1 Reference	281.267	1	5	1.793	0

Table 5. ADME parameters for the selected compounds and the references.

Title	CNS ^a	QPlogS ^b	QPPCaco ^c	QPlogBB ^d	QPPMDCK ^e
Paraconfurane L (51)	-2	-4.161	116.757	-2.165	48.55
Paraconfurane I (48)	-2	-1.869	221.044	-1.569	96.785
Paraconfurane J (50)	-2	-3.251	108.798	-2.08	44.983
1-(1',2'-Dideoxy- α -D-nucleopyranosyl)- β -carboline (73)	-2	-2.059	143.554	-1.874	60.699
1-Acetyl- β -carboline (75)	-2	-3.513	69.826	-1.164	35.425
LasR Reference	-2	-1.97	310.908	-1.431	259.182
KEAP1 Reference	-2	-3.038	35.651	-1.333	17.13
Acceptable ranges	-2 in active to +2 active	-6.5-0.5	<25 poor >500 great	-3-1.2	<25 poor >500 great

^aPredicted CNS activity; ^bPredicted aqueous solubility, log S. S in mol dm⁻³ is the concentration of the solute in a saturated solution that is in equilibrium with the crystalline solid.; ^cPredicted apparent Caco-2 cell permeability. Caco2 cells are a model for the gut-blood barrier. QikProp predictions are for nonactive transport.; ^dPredicted brain/blood partition coefficient. ^ePredicted apparent MDCK cell permeability.; MDCK cells are considered to be a good mimic for the BBB. ^fPredicted human oral absorption on a 0 to 100% scale. The prediction is based on a quantitative multiple linear regression model.

Table 6. Toxicity prediction for the selected compounds and the references.

Title	Cytotoxicity		carcinogenicity		hepatotoxicity		immunogenicity		Mutagenicity	
	Activity	Probability	Activity	Probability	Activity	Probability	Activity	Probability	Activity	Probability
Paraconfurane L (51)	Inactive	0.51	Inactive	0.63	Inactive	0.92	Active	0.98	Inactive	0.73
Paraconfurane I (48)	Inactive	0.61	Inactive	0.75	Inactive	0.86	Inactive	0.96	Inactive	0.66
Paraconfurane J (50)	Inactive	0.54	Inactive	0.78	Inactive	0.89	Active	0.73	Inactive	0.75
1-(1',2'-Dideoxy- α -D-nucleopyranosyl)- β -carboline (73)	Inactive	0.8	Inactive	0.81	Inactive	0.74	Inactive	0.91	Inactive	0.61
1-Acetyl- β -carboline (75)	Inactive	0.83	Inactive	0.77	Inactive	0.56	Inactive	0.96	Inactive	0.79
2UV0_LasR_Ref	Inactive	0.67	Inactive	0.61	Inactive	0.73	Inactive	0.99	Inactive	0.83
7OFE_KEAP1_Ref	Inactive	0.63	Inactive	0.52	Inactive	0.73	Active	0.55	Inactive	0.58

five states that the mol_MW should be less than 500, QPlogPo/w should be less than 5, and the number donorHB should be no more than 5, the number of acceptHB should be no more than 10, and QPlogPo/w should be between -2 and 6.5. Based on these criteria, the compounds are considered drug like, as they satisfy the rule of five.

In addition to the previously mentioned ADME properties, other important factors were calculated and found to be within acceptable ranges, as shown in Table 5. The compounds, as well as the reference, do not penetrate the

blood-brain barrier (BBB), indicating that they are less likely to cause CNS side effects. Regarding solubility, the compounds exhibit good aqueous solubility within the range of -1.8 to -4.1, which is favorable for drug development. Absorption studies showed moderate human oral absorption percentages ranging from 52% to 76%, suggesting that these compounds have the potential to be absorbed efficiently when taken orally. In terms of distribution, the compounds demonstrated moderate permeability to Caco-2 and MDCK cell monolayers. The permeability values ranged from 108 to 310 (Caco-2) and

34 to 259 (MDCK). These values indicate that the compounds have the ability to distribute adequately within the body. On the other hand, the reference compound used in KEAP1 docking showed poor Caco-2 and MDCK permeability as well as poor absorption. This suggests that the reference compound may have limitations in terms of its bioavailability and distribution. Overall, based on their ADME properties, the compounds have the potential to act as drug-like molecules.

Regarding toxicity all the compounds show no toxicity except for compounds (50) and (51) and KEPA1 reference which show immunotoxicity, also all the compounds were in toxicity class between 4 to 5 which is moderate as detailed in Table 6.

CONCLUSION

Fungi have a marked significance as a resource for various bio-metabolites and enzymes, in addition to their applications in industrial, pharmaceutical, and agricultural fields. *Paraconiothyrium brasiliense* has the capacity to produce different classes of metabolites, including Sesquiterpenoids with variable structural frameworks such as bergamotane-, bisabolene-, and eremophilane-types are the major constituents reported from this fungus. In addition, octahydro-naphthalenes, furanones, anthraquinones, xanthenes, iso-coumarins, and alkaloids, as well as other constituents were separated from *P. brasiliense* isolated from endophytic, insect, and sea sediments.

Some of these metabolites were assessed for anti-HIV-1, cytotoxic, anti-hyperglycemic, anti-platelet aggregation, neuroprotective, immunosuppressive, antioxidant, and xanthine oxidase inhibition activities. *Paraconiothyrium brasiliense* produces and induces the production of an anticancer agent, taxol. It has the capacity to produce extracellular enzymes: avicelase, amylase, laccase, β -glucosidase, xylanase, and protease. However, *P. brasiliense* biotechnological potential warrants further investigation to explore its capacity for the production of various enzymes. This *in silico* study, which integrates docking and ADMET prediction, focused on two proteins, KEAP1 and LasR. Compounds 48, 50, and 51 exhibited remarkable binding affinity for KEAP1, forming crucial interactions, indicating their potential mechanism as promising neuroprotective agents. In addition, some compounds showed notable binding affinity for LasR raising the possibility of undiscovered antibacterial properties. Moreover, ADMET predictions reveal that these compounds possess a favorable toxicity profile and exhibit desirable drug-like characteristics, positioning them as potential candidates for drug development.

AUTHOR CONTRIBUTIONS

Conceptualization, SRMI and GAM; methodology, SRMI, GAM, AAA, and FAE; software, AAA, SME, AAF, AHEH, Structures drawing and tables construction, AEK, AHA, WO, AA, SME, AAF, AHEH; data curation, AEK, AHA, WO, AA, IAS; writing original draft preparation, SRMI, AAA, and GAM; writing review and editing, WO, AA, SME, AAF, IAS, and AHEH, All authors have read and agreed to the published version of the manuscript.

FINANCIAL SUPPORT

The authors received no external funds or financial support for this article.

CONFLICTS OF INTEREST

The authors report no financial or any other conflicts of interest in this work.

ETHICAL APPROVALS

This study does not involve experiments on animals or human subjects.

DATA AVAILABILITY

All the data is available with the authors and shall be provided upon request.

CONSENT FOR PUBLICATION

All authors have read and approved the final manuscript.

USE OF ARTIFICIAL INTELLIGENCE (AI)-ASSISTED TECHNOLOGY

The authors declares that they have not used artificial intelligence (AI)-tools for writing and editing of the manuscript, and no images were manipulated using AI.

PUBLISHER'S NOTE

All claims expressed in this article are solely those of the authors and do not necessarily represent those of the publisher, the editors and the reviewers. This journal remains neutral with regard to jurisdictional claims in published institutional affiliation.

LIST OF ABBREVIATIONS

A549: human lung adenocarcinoma epithelial cell line; ACS: American Chemical Society; ADMET: absorption, distribution, metabolism, excretion, and toxicity; C8166: human T cell leukaemia; CC: column chromatography; CD: circular dichroism; CNS: central nervous system; EC50: half maximal effective concentration; ECD: electronic circular dichroism; GCMS: gas chromatography mass spectrometry; HIV-1: human immunodeficiency virus; HO8910: human ovarian cancer cell line; HOA: human oral absorption; HRMS: high resolution mass spectrometry; IC50: half-maximal inhibitory concentration; LMP1: latent membrane protein 1; MCF-7: human breast adenocarcinoma cell line; MGC: human gastric cancer cell line; MTT: 3-(4,5-Dimethylthiazol-2-yl)-2,5-diphenyltetrazolium bromide; NIH3T3: mouse embryonic fibroblast cells; NPs: nanoparticles; PANC-1: human pancreas ductal carcinoma cell line; PC12: rat adrenal pheochromocytoma cell line; RBC: red blood corpuscle; RP-HPLC: reversed phase-high-performance liquid chromatography; SDGs: sustainable development goals; Srebf1 sterol regulatory element binding transcription factor 1.

REFERENCES

1. Ryan MJ, McCluskey K, Verkleij G, Robert V, Smith D. Fungal biological resources to support international development: challenges and opportunities. *World J Microbiol Biotechnol.* 2019;35:139.

2. Tennakoon DS, Thambugala KM, Silva NID, Suwannarach N, Lumyong S. A taxonomic assessment of novel and remarkable fungal species in *Didymosphaeriaceae* (*Pleosporales*, *Dothideomycetes*) from plant Litter. *Front Microbiol.* 2022;13:1016285.
3. Kržišnik D, Gonçalves J. Environmentally conscious technologies using fungi in a climate-changing world. *Earth.* 2023;4:69–77.
4. Purahong W, Pietsch KA, Lentendu G, Schöps R, Bruelheide H, Wirth C, *et al.* Characterization of unexplored deadwood mycobiome in highly diverse subtropical forests using culture-independent molecular technique. *Front Microbiol.* 2017;8:574.
5. Hareeri RH, Aldurdunji MM, Abdallah HM, Alqarni AA, Mohamed SG, Mohamed GA, *et al.* *Aspergillus Ochraceus*: metabolites, bioactivities, biosynthesis, and biotechnological potential. *Molecules.* 2022;27:6759.
6. Ibrahim SR, Sirwi A, Eid BG, Mohamed SG, Mohamed GA. Bright side of *Fusarium Oxysporum*: secondary metabolites bioactivities and industrial relevance in biotechnology and nanotechnology. *J Fungi.* 2021;7:943.
7. Ibrahim SR, Mohamed SG, Altyar AE, Mohamed GA. Natural products of the fungal genus *humicola*: diversity, biological activity, and industrial importance. *Curr Microbiol.* 2021;78:2488–509.
8. Saye LM, Navaratna TA, Chong JP, O'Malley MA, Theodorou MK, Reilly M. The Anaerobic fungi: challenges and opportunities for industrial lignocellulosic biofuel production. *Microorganisms.* 2021;9:694.
9. Ibrahim SRM, Choudhry H, Asseri AH, Elfaky MA, Mohamed SGA, Mohamed GA. *Stachybotrys Chartarum*-a hidden treasure: secondary metabolites, bioactivities, and biotechnological relevance. *J Fungi.* 2022;8:504.
10. Ibrahim SRM, Altyar AE, Mohamed SGA, Mohamed GA. Genus *Thielavia*: phytochemicals, industrial importance and biological relevance. *Nat Prod Res.* 2022;36:5108–23.
11. Ibrahim SR, Omar AM, Muhammad YA, Alqarni AA, Alshehri AM, Mohamed SG, *et al.* Advances in fungal phenalenones—natural metabolites with great promise: biosynthesis, bioactivities, and an *in silico* evaluation of their potential as human glucose transporter 1 inhibitors. *Molecules.* 2022;27:6797.
12. Omar AM, Mohamed GA, Ibrahim SR. Chaetomugilins and chaetoviridins—promising natural metabolites: structures, separation, characterization, biosynthesis, bioactivities, molecular docking, and molecular dynamics. *J Fungi.* 2022;8:127.
13. Khayat MT, Mohammad KA, Omar AM, Mohamed GA, Ibrahim SR. Fungal bergamotane sesquiterpenoids—potential metabolites: sources, bioactivities, and biosynthesis. *Mar Drugs.* 2022;20:771.
14. Ibrahim SRM, Mohamed GA, Al Haidari RA, El-Kholy AA, Zayed MF, Khayat MT. Biologically active fungal depsidones: chemistry, biosynthesis, structural characterization, and bioactivities. *Fitoterapia.* 2018;129:317–65.
15. Prescott TA, Hill R, Mas-Claret E, Gaya E, Burns E. Fungal drug discovery for chronic disease: history, new discoveries and new approaches. *Biomolecules.* 2013;13:986.
16. Li H, Chen L, Xiong X, Yang H, Xu B, Liu C, *et al.* Structural elucidation and nuclear magnetic resonance spectral assignments of five new compounds from *Paraconiothyrium brasiliense*. *Magn Reson Chem.* 2013;61:184–92.
17. Verkley G, Dukik K, Renfurm R, Göker M, Stielow JB. Novel genera and species of coniothyrium-like fungi in montagnulaceae (*Ascomycota*). *Persoonia.* 2014;32:25–51.
18. Verkley GJ, da Silva M, Wicklow DT, Crous PW. *Paraconiothyrium*, a new genus to accommodate the mycoparasite *Coniothyrium minitans*, Anamorphs of paraphaeosphaeria, and four new species. *Stud Mycol.* 2004;50:323–5.
19. Arredondo-Santoyo M, Vázquez-Garcidueñas MS, Vázquez-Marrugo G. Identification and characterization of the biotechnological potential of a wild strain of *Paraconiothyrium* sp. *Biotechnol Prog.* 2018;34:846–57.
20. Xu G, Mi J, Yang T, Wu L, Yuan X, Li G. Two new polyketide metabolites isolated from *Paraconiothyrium brasiliense*. *Chem Nat Compd.* 2017;53:870–73.
21. Colombier M, Alanio A, Denis B, Melica G, Garcia-Hermoso D, Levy B, *et al.* Dual invasive infection with *Phaeoacremonium parasiticum* and *Paraconiothyrium cyclothyrioides* in a renal transplant recipient: case report and comprehensive review of the literature of *Phaeoacremonium* Phaeohyphomycosis. *J Clin Microbiol.* 2015;53:2084–94.
22. Wang W, Shi Y, Liu Y, Zhang Y, Wu J, Zhang G, *et al.* Brasilterpenes A-E, bergamotane sesquiterpenoid derivatives with hypoglycemic activity from the deep sea-derived fungus *Paraconiothyrium brasiliense* HDN15-135. *Mar Drugs.* 2022;20:338.
23. Afshan NUS, Mujahid U, Ishaq A, Khalid AN. First report of leaf spot of *Sarcococca Saligna* caused by *Paraconiothyrium brasiliense* in Pakistan. *J Plant Pathol.* 2020;102:561.
24. Liu H, Zhang Y, Chen J. Whole-Genome sequencing and functional annotation of pathogenic *Paraconiothyrium brasiliense* causing human cellulitis. *Hum Genomics.* 2013;17:65.
25. Liu L, Gao H, Chen X, Cai X, Yang L, Guo L, *et al.* Brasilamides A–D: sesquiterpenoids from the plant endophytic fungus *Paraconiothyrium brasiliense*. *Eur J Org Chem.* 2010;2010:3302–6.
26. Guo Z, Ren F, Che Y, Liu G, Liu L. New bergamotane sesquiterpenoids from the plant endophytic fungus *Paraconiothyrium brasiliense*. *Molecules.* 2015;20:14611–20.
27. Wang W, Shi Y, Liu Y, Zhang Y, Wu J, Zhang G. *et al.* Brasilterpenes A–E, bergamotane sesquiterpenoid derivatives with hypoglycemic activity from the deep sea-derived fungus *Paraconiothyrium brasiliense* HDN15-135. *Mar Drugs.* 2022;20:338.
28. Nakashima K, Tomida J, Hirai T, Kawamura Y, Inoue M. Paraconiothins A–J: sesquiterpenoids from the endophytic fungus *Paraconiothyrium brasiliense* ECN258. *J Nat Prod.* 2019;82:3347–56.
29. Liu C, Wang L, Chen J, Guo Z, Tu X, Deng Z, *et al.* Paraconfuranones A–H, eight new furanone analogs from the insect-associated fungus *Paraconiothyrium brasiliense* MZ-1. *Magn Reson Chem.* 2015;53:317–22.
30. Liu C, Yu X, Guo Z, He H, Tu X, Deng Z, *et al.* Structural elucidation and NMR spectral assignments of paraconfuranones I–M from the insect-associated fungus *Paraconiothyrium brasiliense*. *Magn Reson Chem.* 2016;54:916–21.
31. Ji-Hui Z, Xin-Lei Y, Meng T, Hui LI, Zhao-Xia L, Cheng-Xiong L, *et al.* Study on β -carboline alkaloids produced by endophytic fungus *Paraconiothyrium brasiliense* and their xanthine oxidase inhibitory activity. *Nat Prod Res Develop.* 2021;33:41.
32. Sathiyaseelan A, Saravanakumar K, Mariadoss AVA, Kim KM, Wang M. Antibacterial activity of ethyl acetate extract of endophytic fungus (*Paraconiothyrium brasiliense*) through targeting dihydropteroate synthase (DHPS). *Process Biochem.* 2021;111:27–35.
33. Liu L, Chen X, Li D, Zhang Y, Li L, Guo L, *et al.* Bisabolane sesquiterpenoids from the plant endophytic fungus *Paraconiothyrium brasiliense*. *J Nat Prod.* 2015;78:746–53.
34. Zhang Y, Zhang Z, Wang B, Liu L, Che Y. Design and synthesis of natural product derivatives with selective and improved cytotoxicity based on a sesquiterpene scaffold. *Bioorg Med Chem Lett.* 2016;26:1885–8.
35. Sathiyaseelan A, Saravanakumar K, Naveen KV, Han, K, Zhang X, Jeong MS, *et al.* Combination of *Paraconiothyrium brasiliense* fabricated titanium dioxide nanoparticle and antibiotics enhanced antibacterial and antibiofilm properties: a Toxicity Evaluation. *Environ Res.* 2022;212:113237.
36. Garyali S, Kumar A, Reddy MS. Diversity and antimutagenic activity of taxol-producing endophytic fungi isolated from Himalayan Yew. *Ann. Microbiol.* 2014;64:1413–22.

37. Shasmita NRS, Rath SK, Behera S, Naik SK. *In vitro* secondary metabolite production through fungal elicitation: an Approach for sustainability. Singapore: Fungal Nanobionics: Principles and Applications, Springer; 2018, pp 215–42.
38. Salehi M, Moieni A, Safaie N, Farhadi S. Elicitors derived from endophytic fungi *Chaetomium globosum* and *Paraconiothyrium brasiliense* enhance paclitaxel production in *Corylus Avellana* cell suspension culture. *Plant Cell Tiss. Organ Cult.* 2019;136:161–71.
39. Choi MA, Park SJ, Ahn GR, Kim, SH. Identification and characterization of *Paraconiothyrium brasiliense* from garden plant *Pachysandra Terminalis*. *Kor J Mycol.* 2014;42:262–68.

How to cite this article:

Ibrahim SRM, Alzain AA, Elbadwi FA, Koshak AE, AlSaedi AH, Ashour A, Osman W, Sindi IA, El-Sayed SM, Farahat AA, Hassan AHE, Mohamed GA. Shedding light on *Paraconiothyrium brasiliense*: Secondary metabolites, biological activities, and computational studies. *J Appl Pharm Sci*, 2024; 14(10):035–052.